ORNL/TM-2018/1059

Crashworthiness Models for Automotive Batteries

A Report on the Department of Energy Project 2088-A031-15 for the National Highway Traffic Safety Administration (NHTSA), an Office of the U.S. Department of Transportation.

Sergiy Kalnaus
Hsin Wang
Abhishek Kumar
Srdjan Simunovic
Srikanth Allu
Sarma Gorti
John A. Turner

OAK RIDGE NATIONAL LABORATORY
MANAGED BY UT-BATTELLE FOR THE US DEPARTMENT OF ENERGY

December 2018

Computational Sciences and Engineering Division (CSED)
Materials Science and Technology Division (MSTD)

Crashworthiness Models for Automotive Batteries

A Report on the Department of Energy Project 2088-A031-15

for the

National Highway Traffic Safety Administration (NHTSA)

an Office of the

U.S. Department of Transportation (DOT)

Sergiy Kalnaus
Hsin Wang
Abhishek Kumar
Srdjan Simunovic
Srikanth Allu
Sarma Gorti
John A. Turner

Date Published:
December 2018

Prepared by

OAK RIDGE NATIONAL LABORATORY

Oak Ridge, TN 37831-6283

managed by

UT-BATTELLE, LLC

for the

US DEPARTMENT OF ENERGY

under contract DE-AC05-00OR22725

Crashworthiness models for automotive batteries

Report on the Department of Energy Project 2088-A031-15 for the National Highway Traffic Safety Administration (NHTSA), an Office of the U.S. Department of Transportation.

Sergiy Kalnaus, Hsin Wang, Abhishek Kumar, Srdjan Simunovic, Srikanth Allu, Sarma Gorti, John A. Turner

Summary

Safety is a key element of any device designed to store energy. Electrochemical batteries convert energy of chemical reactions to electrical energy. Safety considerations are especially important when applied to large automotive batteries designed for propulsion of electric vehicles (EV). The high amount of energy stored in EV battery packs translates to higher probability of fire in case of severe deformation of battery compartment due to automotive crash or impact caused by road debris. While such demand for safety has resulted in heavier protection of battery enclosure, the mechanisms leading to internal short circuit due to deformation of the battery are not well understood even on the level of a single electrochemical cell. Moreover, not all internal shorts result in thermal runaway, and thus a criterion for catastrophic failure needs to be developed.

This report summarizes the effort to pinpoint the critical deformation necessary to trigger a short via experimental study on large format automotive Li-ion cells subjected to large deformations as those occurring in deformation of battery module or pack. Mechanical properties of cell components were determined via experimental testing and served as input for constitutive models of Finite Element (FE) analysis. It has been rationalized that long-range stress fields occurring in spherical indentation of battery modules would trigger different deformation and failure scenarios compared to indentation of a single cell supported by a rigid flat surface. In order to investigate large deformations characteristic of battery module, a custom experimental set up has been built where the pouch cell was deformed against a compliant backing, which was represented by a ballistic clay. Experiments were also conducted on stacks of 10 pouch cells, -configuration representing half-module in Ford Focus EV battery back. Comparison of the results shows promise for the compliant backing setup for safety evaluation of battery cells under more realistic conditions compared to indentation of single cell against undeformable backing where compression and electrode particle penetration through separator could be the major mechanism for short circuit.

Contents

Introduction

Li-ion batteries for mobile electronic devices and appliances are usually in the form of single cells or small cell packs, where mechanical abuse could occur by handling of the cells during transportation and storage. The end-users are not subjected to risks from mechanical abuse under normal conditions. Although the once in several million chance of self-induced internal short circuit event has always been a potential safety concern, recent advances in cell chemistry, safer electrolytes, separators [1], and battery management system (BMS) have kept this issue a low priority. The emphasis on greater specific power for mobile devices has led to current Li-ion cells to share the same designs with a light-weight pouch cell and thinner layers of current collectors and separators. They are vulnerable to mechanical abuses such as crushing, bending and dropping. For electric vehicle (EV) applications, the same designs for small cells were simply scaled up in dimensions to make large format cells. The larger cells carry significantly more energy and also inherit the same mechanical abuse-intolerant characteristics of their smaller counterparts. For the same mechanical damage and same state of charge (SOC), a larger cell is more likely to go to thermal runaway because it has higher capacity and more current can flow through the short circuit spot to trigger thermal runaway. With the increasing number of electrical vehicles entering the active fleet, battery safety has become an important issue [2]. In addition to the safety of handling and transporting the cells, the EV users can be directly affected by the mechanical abuses and failure of the batteries. In order to avoid mechanical damage, the cell packs are located in the crush-safe zones and protected by extra armors. However, severe accidents can still lead to mechanical deformation of the cells, short circuit in the cells and potential thermal runaway.

A damage tolerant design of batteries rests upon detailed understanding of the processes leading to failure and the ability to model such processes. Such understanding is especially critical in the case of battery pack designs for electric vehicles. Current lack of such understanding is not surprising, considering the difficulty of the problem, which combines mechanics of battery response to crush loading with electrical and chemical behavior. While there are federal safety regulations [3] and industry standards related to battery safety [4, 5], they mostly address passive safety measures such as electrolyte spillage or disconnection of the high voltage battery pack in case of malfunction.

A number of tests on safety of Li-ion cells under mechanical abuse has been developed over the years, with probably the most well-known being the “nail penetration tests” standardized by SAE as J2462 [6]. Majority of the recommendations for abuse testing of automotive batteries can be found in “Abuse Test Manual for Electric and Hybrid Electric Vehicle Applications” released by Sandia National Laboratories [7]. It should be mentioned that unavoidable manufacturing variability results in difficulties in the determination of the location of short circuit and formulation of criteria for thermal runaway. In addition, most of the tests are destructive, and post-mortem analysis cannot supply definitive evidence regarding the origin of the short. Localized high Joule heating within the internal short circuit can trigger a chain of exothermic reactions that can raise the temperature enough to create combustion of flammable gases in the cell (thermal runaway).

In the current report we summarize the recent results of experiments and numerical simulations of deformation and failure of pouch cells in battery modules. We study effects of internal inactive module components (i.e. cooling plates and protective enclosure) on mechanical

response and onset of short circuit. We match the experimental results with FE-based numerical simulations incorporating the criterion for failure based on critical strain in the separator, following our previous work. Finally, we demonstrate coupling between mechanics and electrochemical performance of batteries by applying electrochemical cycling to small prismatic cells in the deformed state and measuring resulting changes in capacity. This behavior is matched by an electrochemical model which treats compaction of electrodes due to external loading by applying local changes in porosity. We observe good correlation between experiments and simulation results.

Deformation and failure of cells in battery module

Various studies can be found in the literature on mechanical testing of Li-ion cells [8]. For small cells used in mobile devices, UL 1642 [9] describes four mechanical abuse tests that the cells with less than 5 grams of metallic lithium must pass, including crushing, impact, shock and vibration. These tests mainly focus on possible mechanical abuses during the transportation and storage of the cells. The passing criteria for these tests are: no fire and no explosion. For self-induced internal short circuit, there is no standard test. Most techniques were developed to simulate an internal short circuit at a single layer due to manufacturing defects. Alternative ways to simulate such a defect require opening a live cell and putting a foreign object inside the cell [10] or embedding an "instigator" inside the cell [11, 12]. These methods work well in a laboratory environment and are not practical in production and for in-service evaluations. Nail penetration [13] or single-side indentation [14] usually can cause extensive damage to the cell before the short circuit event. Efforts to develop mechanical pinching [15] and torsion [16] tests have been made to modify the simple nail penetration or mechanical indentation tests in order to induce a small short circuit spot deep inside the cell. It is important to point out that none of the above tests can perfectly mimic an actual internal short circuit event. They can be treated as cell safety evaluation methods and are more effective in comparing cell-to-cell and design differences.

For large format cells, no formal mechanical abuse test standards or internal short circuit tests are available, although many efforts can be found in the literature [17-19]. Mechanical testing to simulate damage in a crash situation is fundamentally different from internal short circuit simulations. These tests need to cover various externally induced mechanical deformations. In most cases, the damage involves multiple layers and in some cases multiple cells. It is common to conduct mechanical deformation tests until battery failure (usually a voltage drop) is detected. The final results are multiple layer short circuit and rapid local heating. Even with the minimal capacity, the resulting mechanical damage and localized Joule heating make it very difficult to pin-point the final failure mechanism. In most accidents involving EVs, the field data are very hard to obtain, and are totally destroyed in the case of vehicle fire. In addition, the vast majority of experiments on mechanical abuse involve testing single cells on rigid foundation, which triggers significant compressive strains and stresses, as well as the possibility for electrode particle penetration through the separator. The latter was standardized into the "mix penetration strength" requirement for battery separators [20]. Deformation inside the battery pack however triggers larger strains and results in a different strain distribution due to coordinated response of multiple cells in a battery.

Studying the behavior of automotive pouch cells in battery modules was the primary goal of this work. Development of an experimental setup that would allow such study was one of the major tasks. Building on our previous efforts within this project we have designed a new and improved setup for testing of large pouch cell modules. In what follows we describe the results from the experiments in the new setup showing remarkable reproducibility of the internal short circuit occurrence at specific displacement. We also report on the criterion for internal short circuit that was developed based on the critical strain measure in the separator. Finite Element simulations employing this criterion displayed excellent correlation with the experimental results.

As in our previous report [21] majority of the experiments were performed utilizing cells from the Ford Focus EV battery pack provided by NHTSA. These are 227x165 mm pouch cells, which were shipped to ORNL in completely discharged condition. This allowed testing of internal short without safety hazards and permitted detailed analysis of the deformation and failure in cells which would have been impossible in charged cells due to thermal runaway. Experiments involving cycling of cells with applied deformation were done on small 30x40 mm prismatic cells of 0.7 Ah capacity.

Experimental setup with ballistic clay

In this section we briefly describe our efforts in the development of a test setup in which we attempted to simulate all but the top pouch cell in a stack with an equivalent material substitute. In particular we considered ballistic clay, which is often used in high speed testing of ballistic armor. Details of the setup with the ballistic clay box have been described in our previous report [21] together with the initial results. Here we report on the additional multiple experiments done with this setup and finalize the conclusions and outcomes of this task.

In preparing the testing conditions we based our procedure on MIL STD 3027 describing ballistic testing of hard body armor. Ballistic clay (Roma plastilina) was warmed slightly (to approximately 40 ^{o}C) and worked into an aluminum box (285.4 x 235.4 mm footprint). The height of the box (60 mm) was designed to represent the thickness of the 10-cell stack. Clay was removed from the box after each test and new clay was used for subsequent experiments. All of the experiments were performed at room temperature and after molding the clay into the test box, it was allowed to “set” for 2 hours prior to testing.

The basic schematic of the electrical connections of the “cell-on-clay” setup is shown in Fig. 1(a). Since the pouch cells were received in fully discharged state, a constant current source was connected to the cell in order to increase its voltage to a level at which short circuit could be clearly detected (usually 1 V was sufficient). The box with the cell was covered by a top plate which had a circular opening for the spherical indenter; the latter was 1 inch in diameter and was attached to the load train of the servo-hydraulic machine (Fig. 1(b)). All of the experiments were done at the displacement rate of 0.127 mm/s. More details of the experimental conditions can be found in [21].

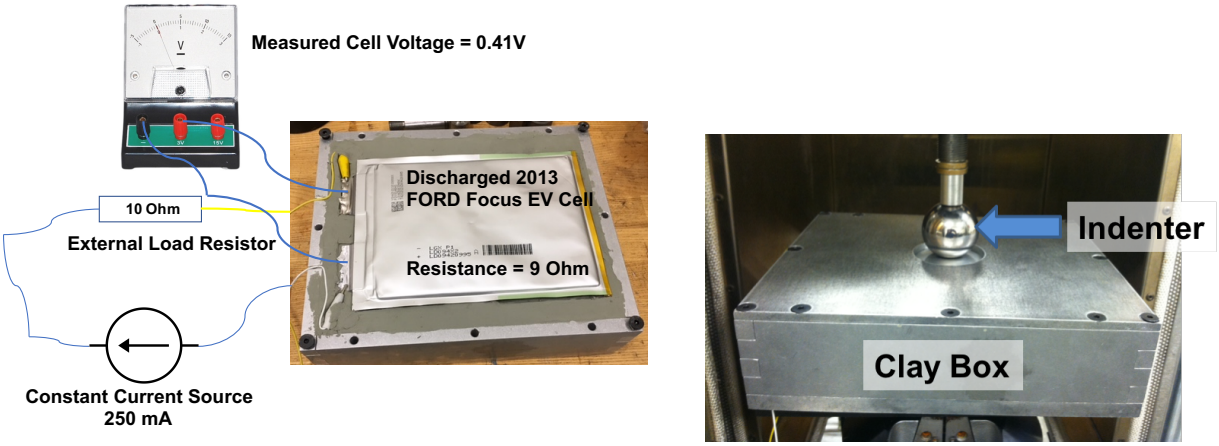

(a) (b)

Fig. 1. Experimental setup for the mechanical testing of pouch cell against ballistic clay: (a) electrical connections; (b) setup in the servo-hydraulic machine.

The results of the all of the experiments are shown in Fig. 2 as load-displacement curves. The locations of short circuit registered by potential drop are marked with asterisks. Overall, the force-displacement curves show multiple points where the loading slope has changed, indicating failure events inside the cell. These events however do not happen at the same displacement magnitude in all of the cells. It can be seen that there is significant amount of scatter when the critical displacement at which internal short circuit occurred is considered. With such a significant scatter of the results, validation of numerical models seems unfeasible. It should also be noted that in four experiments no short circuit was observed - these are marked as "No V Drop" in Fig. 2. The voltage drop however was registered in one of these experiments when the indenter was retracted back. Based on these observations we conclude that failure of the cells happened in tension which allowed the electrodes to form a major tensile crack and drift apart without contact or a short circuit. As the indenter was retracted, the electrodes came into contact and at that moment the potential drop was observed. In our previous report [21] we described and quantified significant difference in stiffness between ballistic clay (of different grades) and the stack of 10 pouch cells. The difference

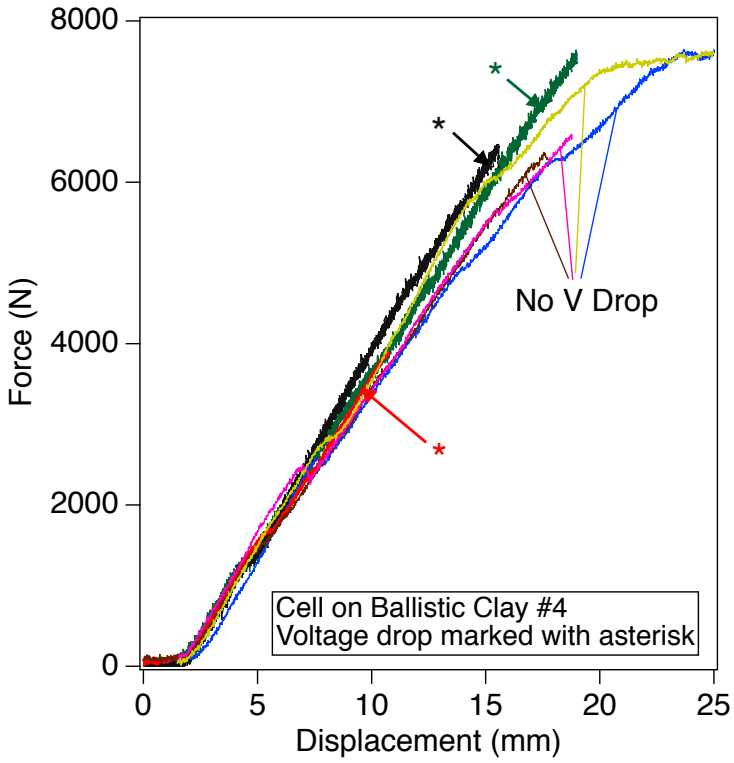

Fig. 2. Results of "cell-on-clay" indentation experiments

in stiffness observed in earlier tests [21], coupled with the variability in the displacement at which internal short circuit was observed, led us to conclude that ballistic clay cannot serve as a reliable substitute for the material representing a stack of cells. We therefore shifted our efforts to experiments with stacks of cells, representing battery modules, so that the mechanical behavior of these systems can be captured accurately. These results will ultimately guide the selection of backing material that may replace ballistic clay in the future.

New experimental setup for battery module

In order to maximize reproducibility of the experimental results we have designed a new setup for indentation of a stack of pouch cells as shown in Fig. 3 [22]. The goal was to achieve precise control of the loading mode of the cell stack. In order to avoid any possible bending of the coupling between the indenting sphere and the load train, which can result in tangential forces being applied to the pouch cell, the sphere was completely detached from the load train. Instead, the die-set setup was constructed in which the sphere was driven into the cell stack through the force applied to a plate, which in turn was guided by four linear bearings (Fig. 3). A small circular groove in the top loading plate ensured positioning of the sphere and force transfer in the direction strictly perpendicular to the cell surface.

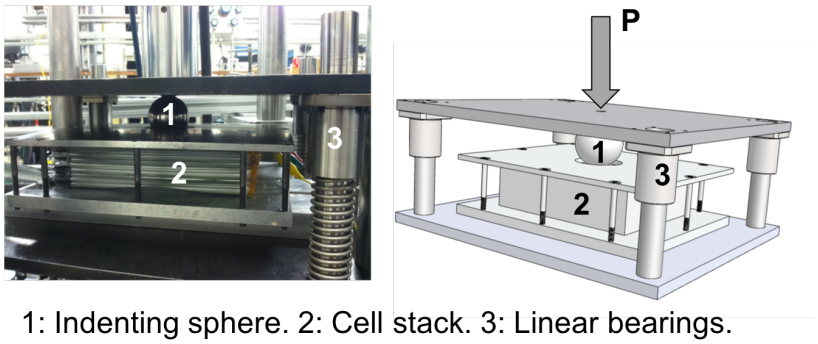

1: Indenting sphere. 2: Cell stack. 3: Linear bearings.

Fig. 3. Die-set with spherical indenter designed for pouch cell stack mechanical testing.

The setup was designed to replicate the conditions inside the battery module consisting of pouch cells. In order to achieve that, the stack of 10 cells representing one half of a Ford Focus EV battery module was sandwiched between two aluminum plates under pressure. The pressure was maintained by 10 screws connecting the upper and lower aluminum plates. The upper plate had an opening to accommodate the spherical indenter. As with the experiments involving ballistic clay, the indentation was controlled by displacement rather than by the force and the rate of the displacement of the indenter was maintained at 0.127 mm/s.

The die-set with the cell stack was installed in an MTS servo-hydraulic loading frame with a 110 KN load cell. All tests started with a 645 N pre-load applied to the hardened steel sphere in order to ensure consistent origin for all of the indentation experiments. Depending on the experiment, either the top cell or the two top cells in the stack were connected independently to the constant current source and their potential was measured synchronously with the force and displacement by the data acquisition channels. As was mentioned in the previous section, passing the small amount of current through the cell was necessary in order to charge it to the level at which the potential drop due to the short circuit can be reliably measured (~ 1.0 - 1.5V). The experiment would be terminated when the potential drop either in the top cell or in the two top

cells was registered, as shown in Fig. 4. All of the tests were conducted at room temperature and in ambient atmosphere.

The results of the experiments on the stacks containing 10 Ford Focus EV pouch cells are shown in Fig. 5. It can be seen that the experiments show remarkable reproducibility with load-displacement curves corresponding to different pouch cell stacks following each other. The points corresponding to the short circuit(s) are indicated with the arrows. In the experiments where potential was monitored in the two top cells, failure in both cells can be recorded independently. It should be mentioned that in one experiment a significant lag between short circuit in top and next to the top cell has been recorded. In all other cases the failure in two top cells occurred nearly simultaneously.

Significant difference in the magnitude of force can be observed when the results from cell stacks are compared to the results of "cell-on-clay" configuration. This is expected, considering much lower stiffness of the ballistic clay compared to that of a stack of pouch cells, as has been demonstrated in the previous report [21]. Overall, the internal failure in the cells under spherical indentation occurred at very consistent displacement of the indenter, close to approximately 10 mm. This consistency will be discussed in detail further in the report, together with other observations and formulation of failure criterion.

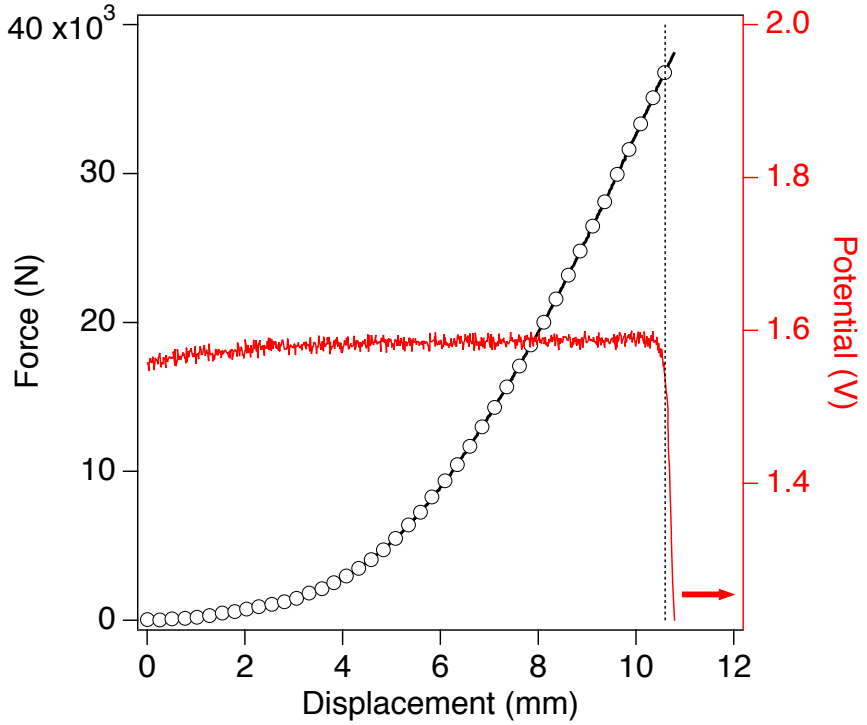

Fig. 4. Detecting internal short circuit using potential drop during the battery cell stack experiments.

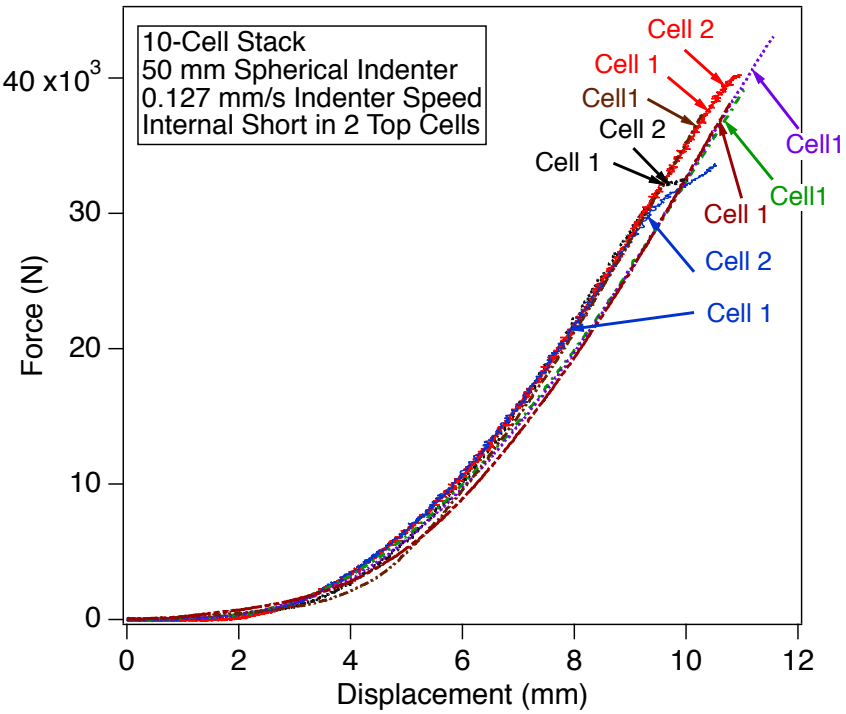

Fig. 5. Force-displacement curves corresponding to indentation of stacks of ten pouch cells. The occurrence of internal short circuit are indicated by the arrows.

Effect of battery module components

EV battery modules contain a number of auxiliary components that do not directly participate in storage and release of electrical charge to the drivetrain. These components may affect the overall mechanical response of the module and alter the failure mode. In order to better simulate the conditions of battery module deformation under external mechanical loading we included inactive module components, such as cooling plates and plastic enclosure, in our consideration and carried out the corresponding experimental program [22].

The pouch cells were extracted from the same Ford Focus EV battery modules utilized throughout this investigation. The full module contains 20 pouch cells and is shown in Fig. 6 (in this module all but one of the cooling plates have been removed). The detailed procedure for the module removal from the battery pack and extraction of cells can be found in [21]. Three components constituting the battery module considered here are pouch cells, cooling plates and the face plate of the module plastic enclosure (Fig. 7). The cells in the module are held in place by plastic framing and two plastic face plates. Since the spherical indentation occurs out of plane with respect to the pouch cells, we only consider the face plate as a component of the module enclosure. The cooling plates in the module are arranged in such a way, that each cell has one surface contacting the cooling plate. The cooling plate itself (Fig. 7) is made of two thin aluminum sheets stamped to form micro-channels and joined together to provide flow of coolant through the channels.

Fig. 6. Ford Focus EV battery module

The components described above were arranged into configurations replicating a half-module of battery cells, i.e. battery stacks containing 10 cells. In order to investigate the influence of inactive components, three scenarios were considered: (i) stack of 10 pouch cells, (ii) cell stack containing 5 cooling plates placed every other cell, (iii) cell stack with cooling plates and the plastic face plate placed on the top of cell stack to replicate the effect of module enclosure. The thickness of the cell, cooling plate, and plastic face plate was 5.5 mm, 1.3 mm (maximum measured at the cooling channel), and 2.3 mm respectively.

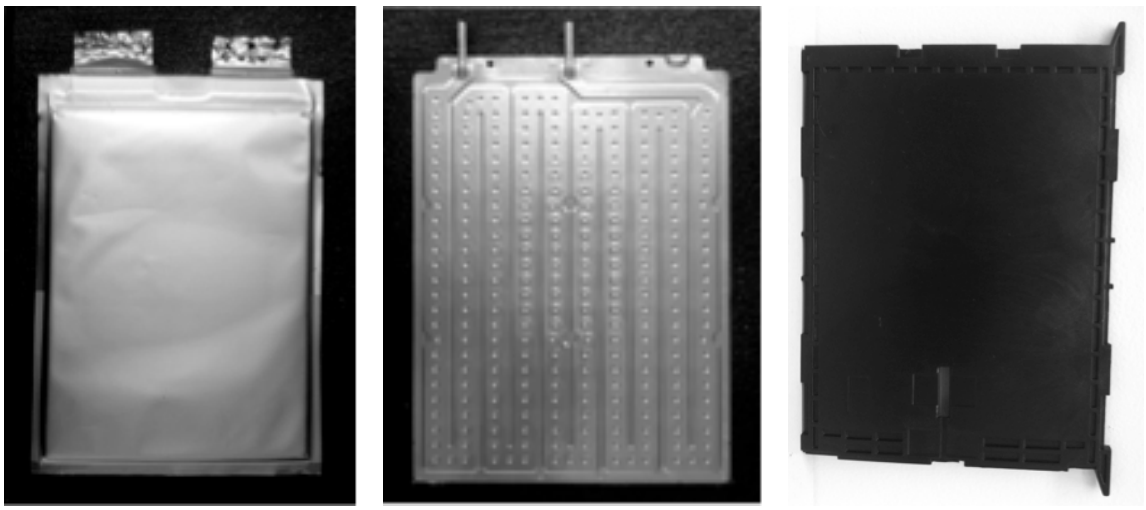

(a) (b) (c)

Fig. 7. Components of the battery module: (a) pouch cell; (b) cooling plate; (c) plastic plate.

The setup was identical to the one described in Fig.3. The die-set was installed in the MTS servo-hydraulic loading frame with 110 kN load cell. The experiments were performed under displacement control with the rate of 0.127 mm/s. The tabs of the top cell were connected to the

data acquisition channel in order to monitor the cell potential as the indentation progressed. As was mentioned earlier, the vehicle battery was delivered to ORNL in completely discharged state and therefore a small current was passed through the top cell in order to increase its potential to approximately 1 V, which allowed for accurate detection of potential drop due to the internal short circuit.

The results of experiments in the form of load-displacement curves are shown in Fig. 8. Each configuration was tested twice to ensure reproducibility of the force-displacement response. The points when internal short circuit was observed in the top cell are marked with asterisk. Similarly to the other tests on battery cell stacks (Fig. 5), remarkable consistency of displacement at which the top cell fails has been observed. This critical displacement appears to be unaffected by the presence of cooling plates and plastic enclosure in the structure. No significant load drop at the point of internal short circuit was observed, which is also similar to the results of other tests on 10-cell stacks, where only a small change in force-displacement curve slope was registered at short circuit (Fig. 5). An interesting observation can be made from Fig. 8: introduction of cooling plates into the module structure reduced the force of indentation. This reduction in force is rather noticeable and is approximately a factor of 1.5 at the end of the loading. We believe that this reduction comes from two factors: (i) collapse of cooling channels of the aluminum cooling plates, and (ii) yielding in ductile aluminum. Contribution from the latter process is illustrated in the Finite Element modeling section. It can also be noted that the presence of the plastic plate on top of the cell stack did not affect either the mechanical response of the half-module or the critical displacement of the indenter at which the top cell developed short circuit. In fact, this critical displacement remains constant regardless of configuration of cell stack and is equal to 10.76 mm (Fig. 8). This important observation allows formulation of a failure criterion based on critical strain, as will be elaborated in the next section.

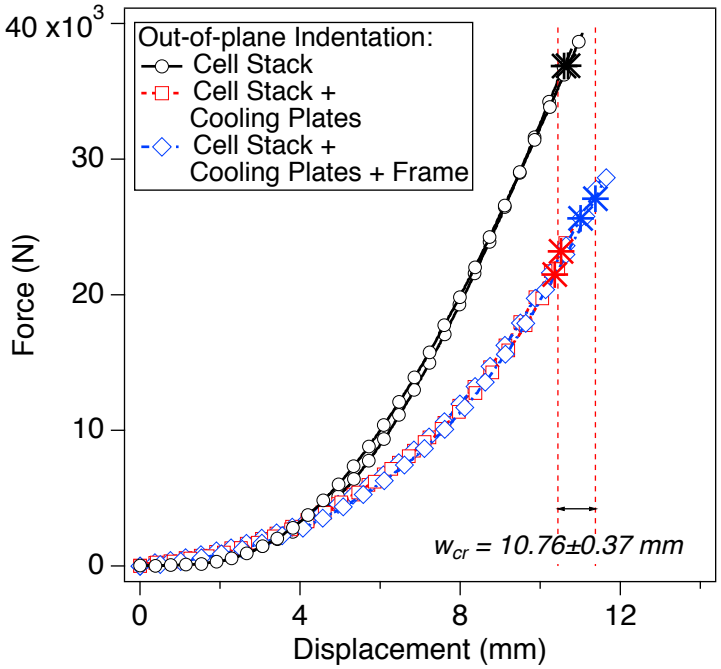

Fig. 8. Results of spherical indentation experiments on battery modules.

Failure criterion based on critical strain and Finite Element simulations

In electrochemical cells, separation of electrodes of opposite polarity is achieved by placing a physical porous barrier between them; this barrier is commonly termed 'separator'. Integrity of the separator plays a key role in prevention of contact between the electrodes that would lead to short circuit. It is therefore a commonly accepted notion that failure of battery separator is the necessary condition for internal short circuit of a battery cell. While overall, ~80% by volume of the cell is composed of electrode active materials, and these active materials develop macroscopic shear cracks dictating the global failure mode (see the next section for details), the actual contact between electrodes is controlled by the local failure of the separator. In our previous efforts [23-25] we have performed a comprehensive experimental program on battery separators of different types. Experiments were performed under different strain rates and temperatures and different types of separators were tested, including the DreamWeaver Gold 40 brand, which is based on non-structured para-amid fiber mats. Our later efforts concentrated on polymer separators, as these represent the vast majority of separators in commercial batteries. In order to study the behavior of commercial polymer separators (manufactured by Celgard) under complex loading conditions representative of deformation scenarios in batteries, we subjected them to a bulge test, which creates a biaxial tensile state in the separator [21, 23]. Strains were measured by digital image correlation technique during the experiment. Since the separators under investigation were manufactured by dry directional stretching, they showed significant anisotropy of mechanical properties in two orthogonal directions (machine direction – MD, and transverse direction – TD). This anisotropy resulted in preferential concentration of strain under biaxial loading, as illustrated in Fig. 9.

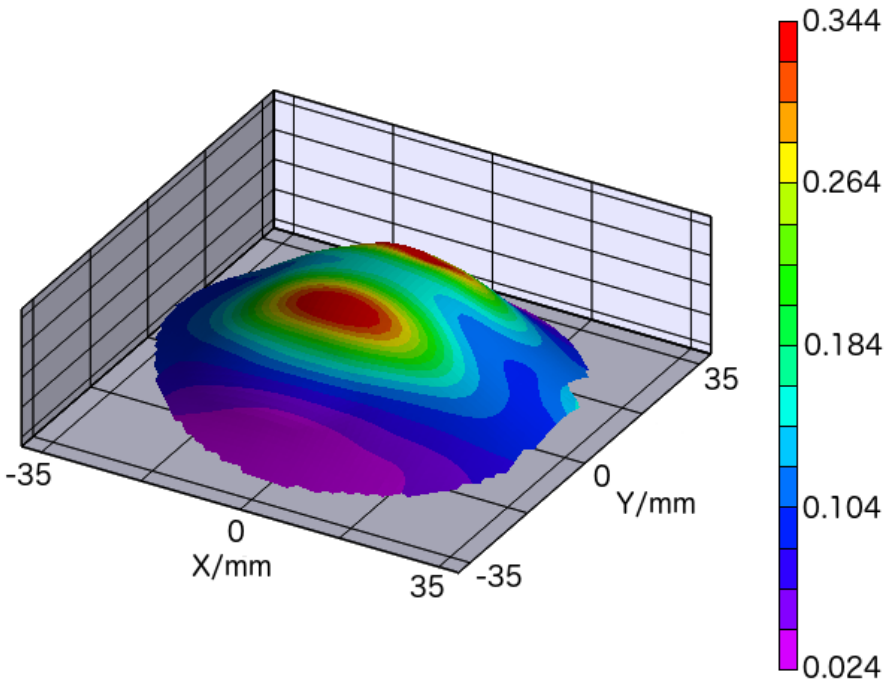

Fig. 9. Example of biaxial deformation of Celgard 2075 polymer separator with mapped major strain.

Two different types of separator were tested and the results of these experiments [21, 23] showed that the separators failed at a consistent first principal strain, which on average was equal to 34%. This strain was found to be independent not only of the separator grade but also of the radius of curvature of the separator under biaxial stretch.

Here we utilize this 34% critical strain criterion in FE analysis of the battery modules in order to predict the occurrence of the internal short circuit during mechanical out-of-plane deformation by a spherical indenter [22]. The FE model includes all 10 cells in the stack and is built to consider two scenarios described in the previous Section: (i) stack of pouch cells and (ii) stack of pouch cells with cooling plates. The corresponding FE meshes are shown in Fig. 10. The Finite Element package LS DYNA was used for the simulations [28]. The indenting sphere was treated as a rigid body. Meshing was performed with solid elements and four cell-sandwich layers were fully resolved in the top cell, with the remaining cells modeled by a representative material (crushable foam – MAT 63 in LS DYNA). Based on our previous investigation, resolving the four top layers was determined sufficient to capture internal short circuit as a result of out-of-plane indentation [29]. Figure 11 shows the schematics of the resolved and homogenized layers within the cell mesh corresponding to the cell stack (Fig. 11a) and cell stack with cooling plates (Fig 11b). The material models used for each of the cell components together with the homogenized material representing the remaining cells in the cell stack are shown in Table 1. The cooling plates were modeled as homogenous isotropic aluminum sheets 0.9 mm thick. This thickness represents an average value between the maximum thickness measured at the cooling channel and minimum thickness where the aluminum sheets are joined together. Creating the mesh of micro-channels for coolant circulation in the aluminum plates would make the problem computationally prohibitive.

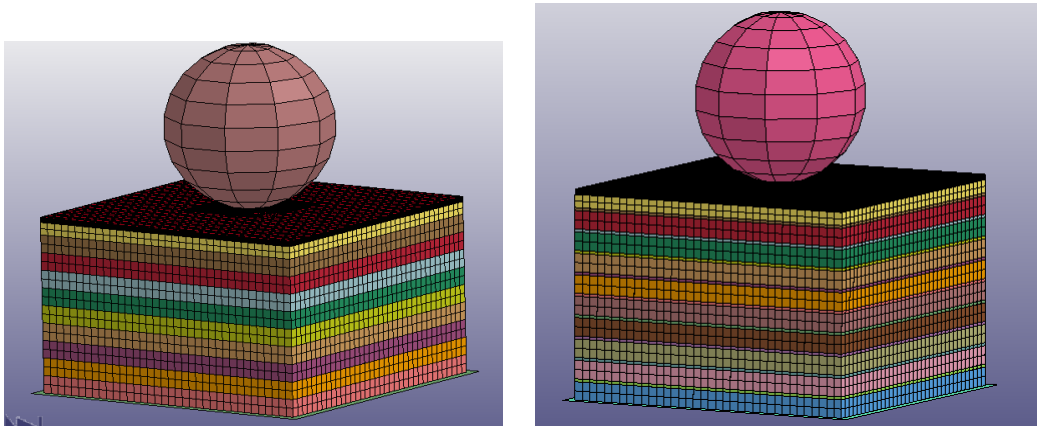

(a) (b)

Fig. 10. Finite element meshes of (a) stack of 10 battery cells; (b) stack of cells with cooling plates.

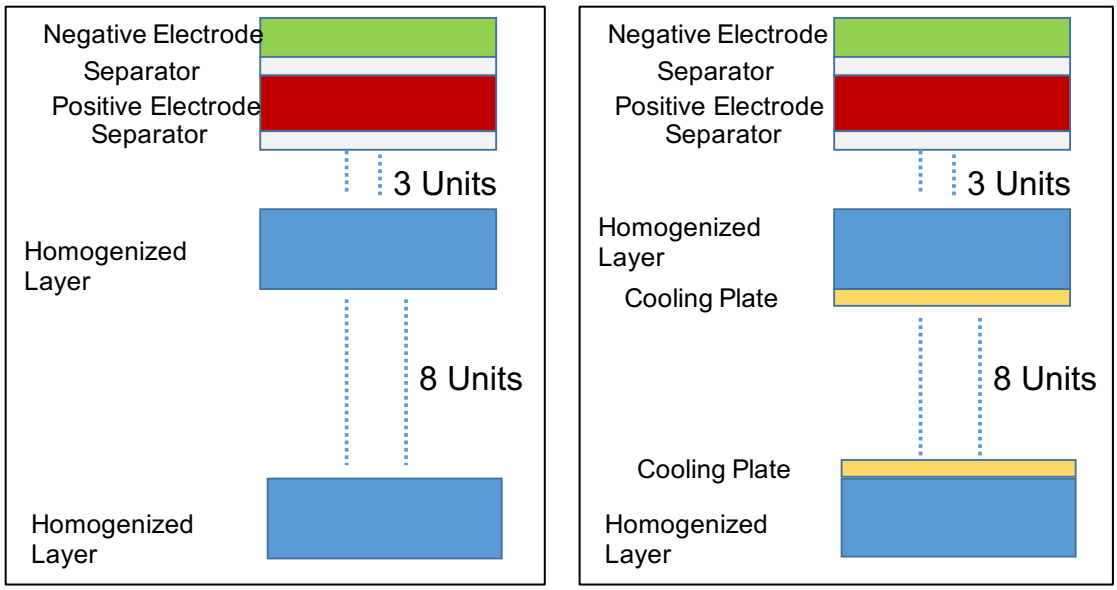

Fig. 11. Schematic of components represented in FE model for: a) 10-cell battery stack; b) 10-cell battery stack with cooling plates (Not to scale).

Table 1. LS Dyna models and basic parameters of each cell component

Component	Thickness mm	LS-Dyna Model	Elastic Modulus GPa	Yield Stress GPa
Anode current collector	0.011	MAT_24	110	0.24
Anode	0.064	MAT_63	0.45	0.04
Separator	0.024	MAT_24	0.50	0.06
Cathode	0.080	MAT_63	0.55	0.04
Cathode current collector	0.018	MAT_24	70	0.24
Homogenized cell material		MAT_63	0.50	0.04

The results of the simulations are compared to the experiments in Fig. 12. Overall good correlation with the experimental results can be observed. The critical strain criterion of $\varepsilon_1 = 0.34$ for the separator failure appears to predict the point of internal short circuit well. In both cases the failure was predicted close to the experimentally observed displacement of the indenter of approximately 11 mm. It can be noticed however that unlike the case of cell stack only, the results of simulations with aluminum cooling plates deviate from the experimental results. While there is a reduction in force captured by the model, this reduction is not as significant as was experimentally observed. This is due to the fact that we did not include cooling channels into our model. The additional decrease in the indentation force can be attributed to the collapse of cooling channels in the aluminum cooling fins, which was not resolved in our model. Despite the above drawback the model predicts correctly the point of voltage drop due to internal short circuit, which is independent of the indentation force.

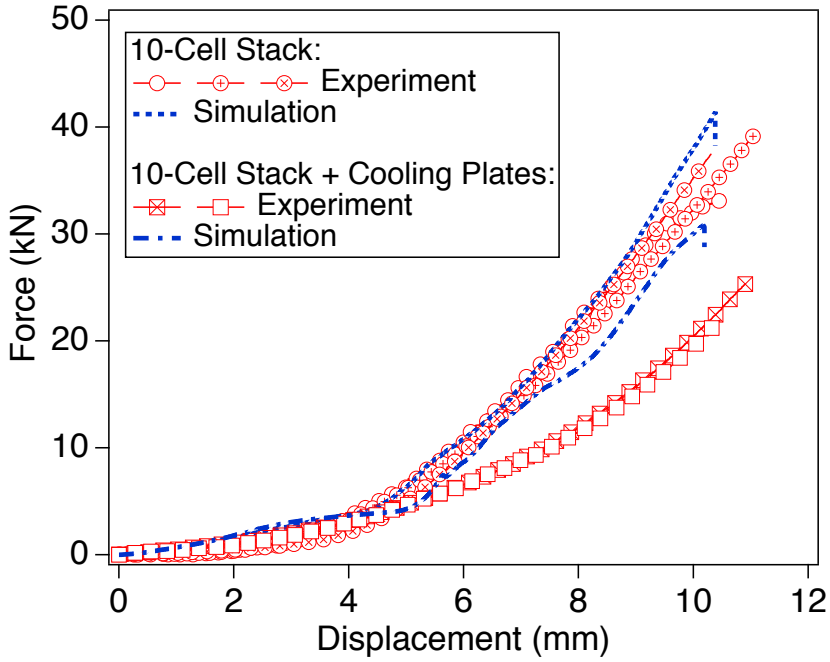

Fig. 12. Comparison between experimentally obtained and numerically predicted load-displacement curves of the cell stack with and without cooling plates.

X-Ray Computed Tomography of cells

Analysis of fracture in the cells was performed by 3D X-Ray computed tomography (CT). The indented cells were cut into 5 cm wide strips with the indented area in the middle. Tapes were used to secure the layers from separating. The indented area was preserved and taken to an X-ray Computed Tomography (XCT) system, Zeiss Versa 520 X-ray, using a tungsten source running at 140 kV/64.4 A max (9W). Two magnifications were used, 0.4X and 4X. The data were collected and reconstructed with Zeiss' Scout and Scan software with further analysis conducted on TXM3DViewer. Schematics showing the part of the cell that underwent imaging together with coordinate system can be found in Fig. 13. The orientation of axes is the same as in all of the XCT images shown in this report.

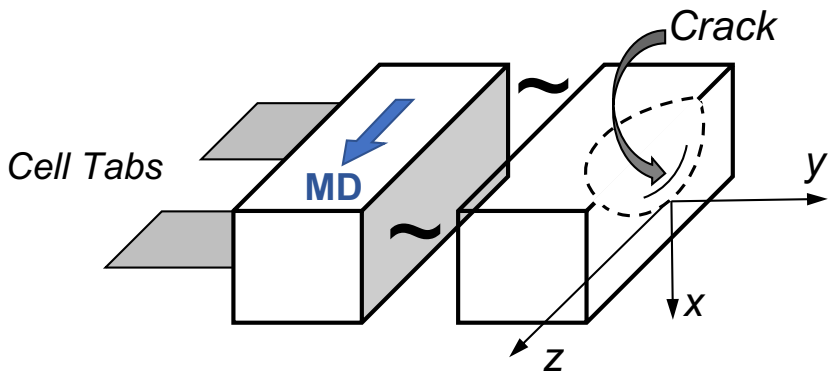

Fig. 13. Schematic showing the coordinate system associated with XCT of pouch cells

Since the cells were in fully discharged state prior to testing, mechanical indentation did not lead to any thermal events and the cells could be further studied after experiments. Non-destructive examination was chosen as the most suitable, since complete disassembly of the cell may unavoidably lead to shifts of electrodes, tears, or delamination of electrode material. The results of the XCT of the top cell of the stack are shown in Fig. 14. Three configurations examined in the current investigation were imaged, and Fig. 14 (a-c) shows failure in top cell of the 10-cell stack, Fig. 14 (d-f) shows failure in stack with cooling plates, and Fig. 14 (g-i) shows cracking in top cell when plastic housing plate was placed on top in addition to cooling plates added to the stack.

Overall it can be seen that the failure mode in the top cell was not influenced by the presence of structural components. All of the cells failed by a major crack oriented at approximately 45^{o}, as can be seen in the *xy*-plane scans. This shear-driven failure most likely displaced the layers of cell electrodes and created sufficient strain to rupture the separator. One critical observation is that the cracks in all of the cells were oriented along the machine direction of the separator, as indicated schematically in Fig. 13. Such preferential failure is consistent with previous observations on failure of dry-processed polymer separators under biaxial tension [21, 23]. This

observation indicates that anisotropic properties of separator influence the configuration of the final failure in the cell.

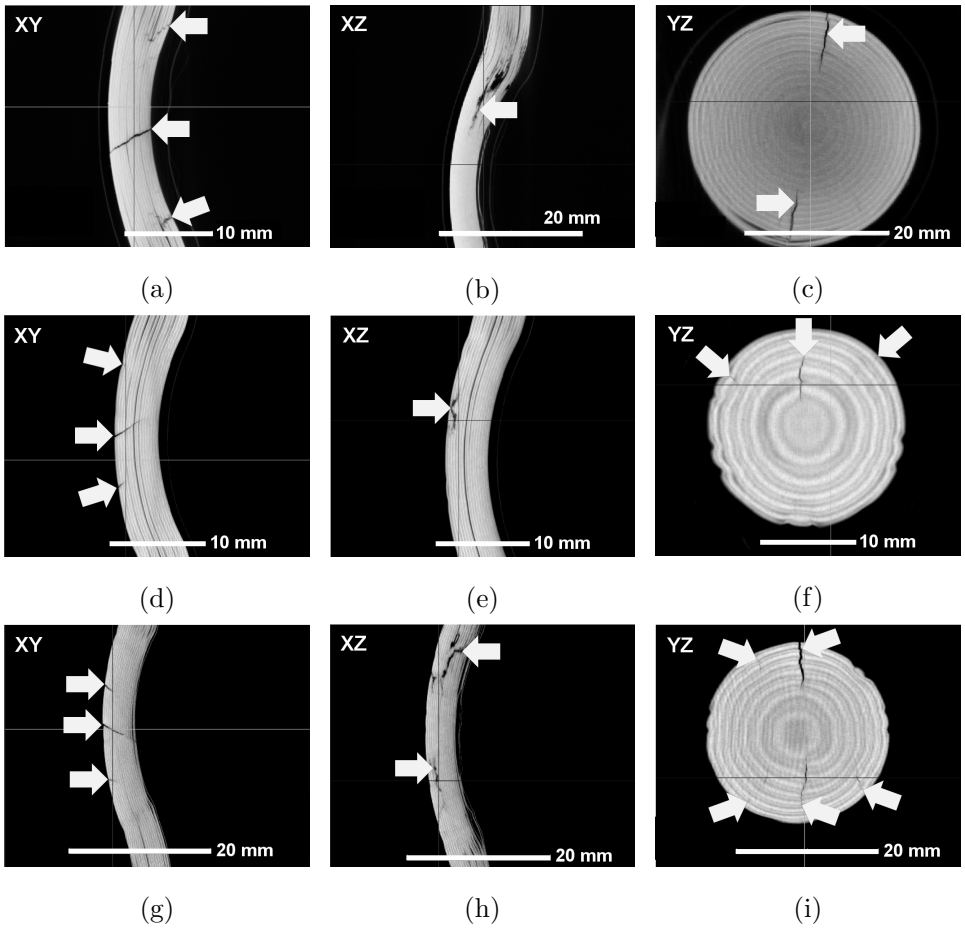

Fig. 14. XCT of the top cell in the stack after failure. (a-c) stack of pouch cells without additional components; (d-f) stack of pouch cells with cooling plates; (g-i) stack of pouch cells with cooling plates and top plastic protective plate.

In several experiments we evolved the indentation past the internal short circuit in the top cell in order to study the propagation of failure in the cell stack. In this case, the potential was monitored independently in the two top cells and the experiment was terminated after the voltage drop was registered in the second cell. In majority of the cases, the delay between the two events was minimal indicating fast propagation of failure once the critical strain has been reached in the top cell. The results are shown in Fig. 15, where the XCT images (a-c) show slip-induced cracks in the top cell of the stack, and images (d-f) demonstrate internal failure in the second from the top cell. Continuous indentation has led to pronounced cracking and shifts of cell layers in the top cell as well as development of additional cracks to accommodate large strains induced by indentation. The failure mode in the underlying cell remains the same – cracking produced by shear slip. This mode is the typical mechanism to accommodate large deformation in bonded particulate systems.

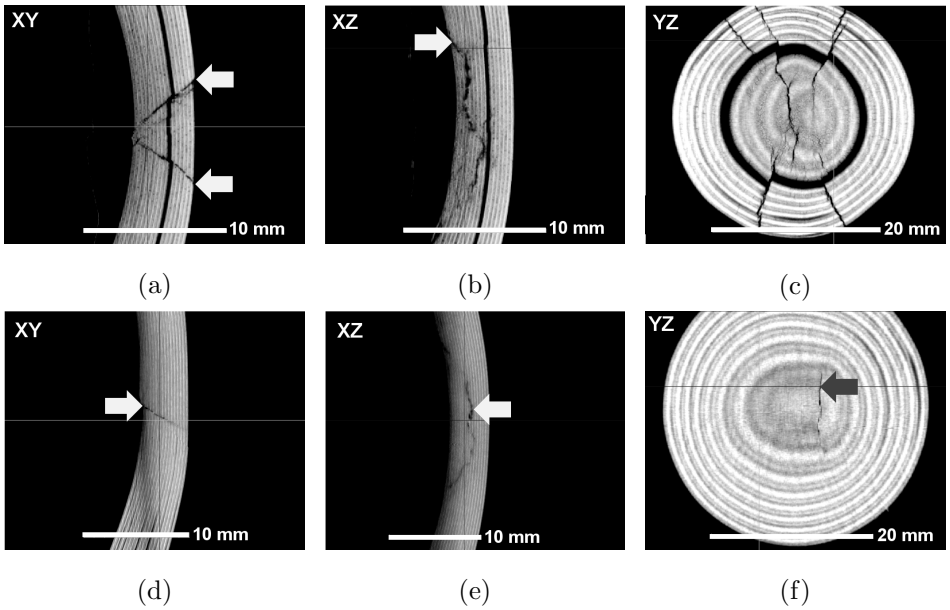

Fig. 15. XCT of the cells indented by the spherical indenter until the short circuit was registered in the top cell of the stack (a-c), as well as the second from the top cell (d-f).

Conclusions

We have developed a new experimental setup and procedures for mechanical testing of EV pouch cell battery modules. In this setup the deformation of pouch cells under conditions representing the battery module can be studied in detail. By isolating module components, we can independently study deformation and failure in a layered structure represented by cells only, as well as to determine the influence of inactive module components by introducing them into the cell stack. As the result, we investigated effects of the protective plastic enclosure of the module and cooling plates placed between the pouch cells in a Ford Focus EV battery pack on forces and critical failure characteristics under transversal indentation by a rigid sphere. The design of the setup together with parameters of servo hydraulic mechanical frame allow for highly controlled experiment in terms of loading mode, displacement rate, and detection of the internal short circuit in the cells. To the best of our knowledge this setup has been proposed for the first time to study mechanics of automotive batteries and can be useful in safety related R&D and safety certification.

We demonstrated that failure in cells leading to internal short circuit can be described by the critical strain criterion, since the failures occurred at a constant displacement of the indenter into the cell stack. This critical displacement was not influenced by the introduction of the cooling plates and plastic module enclosure face plate into the structure. Based on the previous investigation of the mechanics of battery separators, we proposed a failure criterion based on the first principal strain critical value of 34%. This criterion was included in the Finite Element model of the cell stack. The results of numerical simulations followed the experiments very well and accurately predicted the point of internal short circuit. We should mention that this failure criterion is rather approximate since it does not take into account cracking in the electrode layers and consequent rearrangement of stresses. It should be noted that introduction of the cooling plates into the structure noticeably reduced the indentation force, by a factor of approximately 1.5. This is probably due to collapse of cooling channels as well as ductility of aluminum. Further investigation of this effect is required under different loading rates.

To get better understanding of the internal distribution of strain among the layers in the cell and to visualize failure modes we utilized non-destructive evaluation – X-Ray Tomography for the cells following the experiments. It was determined that in all of the cases the failure developed in a slip-like manner, allowing the cell layers to accommodate large strain via shear slip. We propose that such shear slip results in local strains sufficient to cause failure in the separator, which is the necessary condition for the internal short circuit in a battery. The failure mode was not influenced by the presence of the inactive battery components, such as module face plate and cooling plates.

References

[1] J.B. Goodenough and Y. Kim, Chemistry of Materials, 22-3, 2010, 587-603.

[2] L. Hollmotz, M. Hackmann, in: 22nd International Technical Conference on Enhanced Safety of Vehicles (ESV), (2011) 11-0269.

[3] National Highway Traffic Safety Administration (2006). “Electric Powered Vehicles: Electrolyte Spillage and Electrical Shock Protection”, FMVSS No. 305. U.S. DOT.

[4] Kai, X., Xueping, W., et al. (2014). “Comparative research on standards and regulations of electric vehicle post crash safety requirement_Transportation Electrification Asia-Pacific” (ITEC Asia-Pacific), 2014 IEEE Conference and Expo.

[5] SAE International (2014). "Recommended Practice for Electric, Fuel Cell and Hybrid Electric Vehicle Crash Integrity Testing” SAE J1766.

[6] SAE J2464-200911 (2009). “Electric and Hybrid Electric Vehicle Rechargeable Energy Storage System (RESS) Safety and Abuse Testing.” SAE International, Revision 11/06/2009.

[7] SAND 2005-3123 Technical Report (2005). “Freedom CAR Electrical Energy Storage System Abuse Test Manual for Electric and Hybrid Electric Vehicle Applications.” By Doughty, D., and Crafts, C., Sandia National Laboratories http://prod.sandia.gov/techlib/access-control.cgi/2005/053123.pdf

[8] E. Sahraei, J. Meier and T. Wierzbicki, Journal of Power Sources, 220, (2012) 360-372.

[9] UL, in: UL 1642 Standard for Safety for Lithium Batteries, UL, 1999

[10] Battery Association of Japan, Presentation at UN Informal Working Group Meeting, November 11–13, 2008, Washington, DC

[11] M. Keyser, D.Long, Y.S. Jung,A. Pesaran, E. Darcy, B. McCarthy, L. Partrick and C. Kruger, in: Advanced Automotive Battery Conference (AABC), January 25-28, 2011, Panadena, CA

[12] R. Takata, C. McCoy, D. Ofer, R. Stringfellow, B. Barnett and S. Sriramulu, Proceedings of 44th Power Sources Conference, Curran Associates, Inc. Red Hook NY, (2010) p12

[13] J.P. Peres, F. Perton, C. Audry, P. Biensan, A. de Guibert, G. Blanc, M. Broussely, Journal of Power Sources, 97-8 (2001) 702-710

[14] L. Florence, in: Battery Power, Dallas, Texas, 2010, p. 576

[15] W. Cai, H. Wang, H. Maleki, J. Howard, E. Lara-Curzio, Journal of Power Sources, 196 (2011) 7779-7783

[16] F. Ren, T. Cox, H. Wang, Journal of Power Sources, 249 (2014) 156-162

[17] E. Sahraei, R. Hill, T. Wierzbicki, Journal of Power Sources, 201 (2012) 307-321

[18] T. Wierzbicki, E. Sahraei, Journal of Power Sources, 241 (2013) 467-476

[19] R. Spotnitz, R. Muller, The Electrochemical Society Interface, 12 (2012) 57-60

[20] Baldwin, R.S., Bennett, W.R., Wong, E.K., Lewton, M. R., Harris, M.K., Battery separator characterization and evaluation procedures for NASA's advanced lithium-ion batteries, NASA/TM – 2010 – 216099.

[21] Kalnaus, S., Wang, H., Simunovic, S., Kumar, A., Gorti, S.B., Allu, S., Turner, J.A., Crashworthiness models for automotive batteries, (2018), DOI: 10.2172/1435250

[22] Kalnaus, S., Wang, H., Watkins, T.R., Kumar, A., Simunovic, S., Turner, J.A., and Gorney, P., Effect of packaging and cooling plates on mechanical response and failure characteristics of automotive Li-ion battery modules; J Power Sources 403 (2018), 20-26.

[23] S. Kalnaus, A. Kumar, Y. Wang, J. Li, S. Simunovic, J.A. Turner, P. Gorney, "Strain distribution and failure mode of polymer separators for Li-ion batteries under biaxial loading," J Power Sources 378 (2018), 139-145.

[24] Kalnaus, S., Wang, Y., Li, J., Kumar, A., Turner, J.A., Temperature and strain rate dependent behavior of polymer separator for Li-ion batteries; Extreme Mechanics Letters v20, pp. 73-80, 2018.

[25] Kalnaus, S., Wang, Y., Turner, J.A., Mechanical behavior and failure mechanisms of Li-ion battery separators; Journal of Power Sources, v 348, pp. 255-263, 2017.

[26] Barlat, F., Lian, J., Plastic behavior ad stretchability of sheet metals. Part I: a yield function for orthotropic sheets under plane stress conditions, Int J Plast 5 (1989), 51-66.

[27] Lian, J., Barlat, F., Plastic behavior ad stretchability of sheet metals. Part II: effect of yield surface shape on sheet forming limit, Int J Plast 5 (1989),131-147.

[28] "LS-DYNA Keyword User's Manual Volume II Material Models" Version 04/06/16 (r:7556), Livermore Software Technology Company, Livermore, CA, April 2016

[29] Kumar, A., Kalnaus, S., Simunovic, S., Gorti, S.B., Allu, S., Turner, J.A., Communication – indentation of Li-ion pouch cell: Effect of material homogenization on prediction of internal short circuit, J Electrochem Soc, 163(10) (2016), A2494-96.

[30] W. J. Lai, M. Y. Ali, and J. Pan, "Mechanical behavior of representative volume elements of lithium-ion battery cells under compressive loading conditions," *Journal of Power Sources,* Article vol. 245, pp. 609-623, Jan 2014.